Journal of chemical & engineering data

Article

pubs.acs.org/jced

This paper was withdrawn on August 27, 2013

Experimental Measurements and Thermodynamic Modeling of the Dissociation Conditions of Clathrate Hydrates for (Refrigerant + NaCl + Water) Systems

Peterson Thokozani Ngema,[†] Cassandra Petticrew,[†,‡] Paramespri Naidoo,[†] Amir H. Mohammadi,*[,†,§] and Deresh Ramjugernath*[,†]

[†]Thermodynamics Research Unit, School of Chemical Engineering, University of KwaZulu-Natal, Howard College Campus, King George V Avenue, Durban, 4041, South Africa

[‡]OS Engineering, Sasol, PDP Kruger Road, Secunda, 2302, South Africa

[§]Institut de Recherche en Génie Chimique et Pétrolier (IRGCP), Paris Cedex, France

ABSTRACT: Experimental gas hydrate dissociation data for the refrigerants R134a, R410a, and R507 in the absence and presence of NaCl aqueous solutions at various molalities were measured. The binary systems, in this study, which consisted of {chloro(difluoro)methane (R22), or 1,1,1,2-tetrafluoroethane (R134a), or (0.5 mass fraction difluoromethane + 0.5 mass fraction 1,1,1,2,2-pentafluoroethane) (R410a), or (0.5 mass fraction 1,1,1-trifluoroethane + 0.5 mass fraction 1,1,1,2,2-pentafluoroethane) (R507)} + water were measured in the temperature range between (276.4 and 291.8) K and pressures ranging from (0.114 to 1.106) MPa. The ternary system R134a + water + NaCl, at three salt concentrations of (0.900, 1.901, and 3.020) mol·kg^{-1}, was measured in the temperature range between (268.1 and 280.6) K and pressures ranging from (0.086 to 0.383) MPa. For the ternary systems comprising {R410a or R507} + water + NaCl, at two salt concentrations of (0.900 and 1.901) mol·kg^{-1}, measurements were undertaken in the temperature range between (275.1 and 290.3) K and pressures ranging from (0.269 to 1.170) MPa. The isochoric pressure-search method was used to undertake the measurements. The purpose of this study is to generate accurate hydrate phase equilibrium data which will be used to design a wastewater treatment and desalination processes using gas hydrate technology. The results show that the presence of NaCl in the aqueous solutions has a thermodynamic inhibition effect on refrigerant gas hydrates. Modeling of the data measured was undertaken using a combination of the solid solution theory of van der Waals and Platteeuw for the hydrate phase, the Aasberg−Petersen et al. model for the electrolyte aqueous system, and the Peng−Robinson equation of state with classical mixing rules for the liquid and vapor phases. The correlated model results show good agreement with the experimental dissociation data.

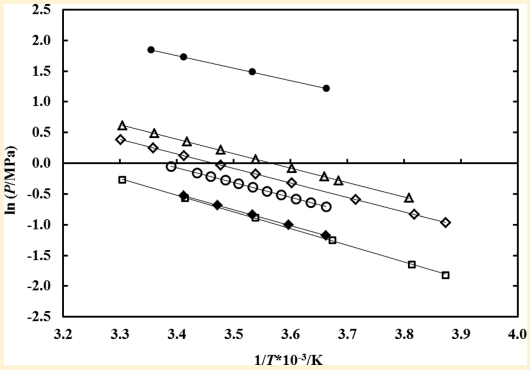

INTRODUCTION

Gas hydrates (or clathrate hydrates) have generally been considered as a nuisance in the petroleum industry, but they have the potential for and have been proposed for many positive applications, for example, wastewater treatment and desalination, CO_2 capture and separation, separation of close-boiling point compounds, hydrogen/methane storage, refrigeration and air conditioning industry, food industry, etc.[1−12] Gas hydrates are solid crystalline compounds physically resembling ice, in which small molecules (typically gases) are trapped inside cages of hydrogen-bonded water molecules.[3] They consist of typically three crystalline structures: structure I (sI), structure II (sII) and structure H (sH) which contain different size and shape cages.[3] The detailed characteristics of these structures can be found in the literature.[3] The large expansion in industrialization and population growth in developed and developing countries has led to a shortage of fresh water.[4,6−8] Seawater, therefore, has become an important source of processed fresh water because it is the most abundant resource on earth.[4,6−8] Reliable and established processes for desalination such as multistage flash (MSF) distillation and reverse osmosis (RO) are generally used to produce fresh water from industrial wastewater and seawater.[4,6−8] Seawater and industrial wastewater contains salts such as NaCl, Na_2SO_4, $MgCl_2$, $CaCl_2$, and $CaSO_4$ which need to be removed from the water.[4,6−8] The processes for the desalination of sea- and wastewater, however, are energy intensive and costly, partly because of the scaling of equipment as a result of saturated sulphates and membrane damage due to the presence of chlorides.[4,6−8] To improve the energy efficiency of desalination processes, it is important to recover water from the concentrated brine solution at ambient temperatures and atmospheric pressure.[4,6−8] Hence, wastewater treatment and desalination using gas hydrate technology has been proposed as an alternative for producing fresh water.[4,6−9]

Javanmardi and Moshefeghian,[4] Eslamimanesh et al.,[9] Chun et al.,[10] and Seo and Lee[11] have reported that the use of refrigerants

Received: January 17, 2013
Accepted: May 13, 2013

   dx.doi.org/10.1021/je400067u | J. Chem. Eng. Data XXXX, XXX, XXX−XXX

for the formation of gas hydrates in water desalination processes is promising when compared to traditional desalination processes. The use of refrigerants to form gas hydrates is attractive because it may enable hydrate formation at ambient conditions. When the gas hydrate dissociates, pure water is potentially produced and the refrigerant released. The refrigerant is then recycled.[12]

Park et al.[7] investigated the removal of salts from seawater using a single stage gas hydrate process. It was found that in a single stage gas hydrate process, (72 to 80) % of each of the dissolved minerals was removed in the following order: $K^+ > Na^+ > Mg^{2+} > B^{3+} > Ca^{2+}$. Chun et al.[10] studied the three-phase equilibria of the chloro-(difluoro)methane (R22), hydrate forming systems in aqueous solutions containing NaCl, KCl, and $MgCl_2$. Hydrate dissociation data were measured at pressures ranging from (0.140 to 0.790) MPa and temperatures between (273.9 and 287.8) K, at several compositions of each the electrolytes. It was found that the addition of electrolytes to the aqueous solutions caused inhibition of the hydrate formation so as to shift the phase disassociation data to lower temperatures.

In this study, accurate gas hydrate phase equilibrium data were measured for the binary systems comprising refrigerant + water and the ternary systems consisting of refrigerant + water + NaCl. The refrigerants studied were 1,1,1,2-tetrafluoroethane (R134a), chloro(difluoro)methane (R22), {0.5 mass fraction difluoromethane + 0.5 mass fraction 1,1,1,2,2-pentafluoro-ethane} (R410a), and {0.5 mass fraction 1,1,1-trifluoroethane + 0.5 mass fraction 1,1,1,2,2-pentafluoroethane} (R507). Measurements for the ternary system[5] were conducted at various concentrations of sodium chloride (the main salt found in brine). The R134a + water + NaCl system was measured at salt concentrations of (0.900, 1.901, and 3.020) mol·kg^{-1}, while the {R410a or R507} + water + NaCl system was measured at salt concentrations of (0.900 and 1.901) mol·kg^{-1}. The binary system of R22 + water was measured in the absence of salt. The range of gas hydrate dissociation conditions for all experiments is summarized in Table 1. The experimental dissociation data were well correlated using the Aasberg-Petersen et al.[13] model for electrolyte aqueous systems with the solid solution theory of van der Waals and Platteeuw[14] used to model the hydrate phase and the Peng−Robinson[15] equation of state with classical mixing rule used for the aqueous/liquid and vapor phases.

Table 1. Salt Concentration, Temperature, and Pressure Ranges Investigated for Hydrate Dissociation Condition Measurements (w_i = Molality of Salt in Aqueous Solution)

hydrate former	salt	w_i	T/K	P/MPa
R22	no salt		278.9 to 288.3	0.181 to 0.645
R410a	no salt		281.2 to 291.8	0.226 to 1.106
	NaCl	0.900	280.5 to 290.3	0.287 to 1.112
		1.901	278.8 to 289.1	0.303 to 1.170
R507	No salt		276.4 to 282.8	0.159 to 0.549
	NaCl	0.900	276.9 to 281.4	0.269 to 0.625
		1.901	275.1 to 279.3	0.289 to 0.656
R134a	no salt		277.1 to 283.0	0.114 to 0.428
	NaCl	0.900	274.6 to 280.6	0.098 to 0.383
		1.901	272.6 to 277.1	0.117 to 0.340
		3.020	268.1 to 273.4	0.086 to 0.299

EXPERIMENTAL SECTION

Materials. The purities of the chemicals used in this study, along with the chemical supplier details are reported in Table 2. A Shimadzu 2010 gas chromatograph (GC) equipped with a thermal conductivity detector was used to check the purities of the refrigerants. The column used in the GC was a Porapak Q. Ultrapure Millipore Q water was used in all the experiments. It had an electrical resistivity of 18 MΩ·cm.[16] NaCl aqueous solutions were prepared using the gravimetric method. An accurate analytical balance (Ohaus Adventurer balance, model no. AV 114) with an uncertainty of ± 0.00005 g was used to prepare the aqueous solutions.[17,18]

Table 2. Purities, Critical Properties, and Suppliers of Refrigerant Studied

chemicals	formula	supplier	purity[f] (mass fraction)	T_c/K	P_c/MPa	acentric factor
water	H_2O	UKZN	1.000	647.14[a]	22.064[a]	0.344[a]
R507	0.5 CHF_2CF_3 + 0.5 CH_3CF_3[e]	Afrox	0.998	343.96[b]	3.797[b]	0.304[b]
R134a	CF_3CH_2F	Afrox	0.999	374.18[c]	4.057[c]	0.326[c]
R410a	0.5 CH_2F_2 + 0.5 CHF_2CF_3[e]	Afrox	0.998	345.65[d]	4.964[d]	0.279[d]
R22	$CHClF_2$	Afrox	0.997	369.26[a]	4.986[a]	0.221[a]
sodium chloride	NaCl	Merck	0.990			

[a]Reference 22. [b]Reference 23. [c]Reference 24. [d]Reference 25. [e]Mass fraction. [f]As stated by the supplier. Checked by GC analysis for the gases and liquids.

Equipment. Figure 1 shows a schematic diagram of the apparatus[16] used in this study. The cylindrical cell was constructed using stainless steel and can withstand pressures up to 20 MPa. The volume of the cell is approximately 60 cm^3. A U-shape magnet which is driven by an overhead stirrer is installed under the cylindrical cell. A magnetic stirrer bar was placed inside the cylindrical cell and, via magnetic coupling with the U-shaped magnet, enabled agitation of the contents. Two platinum resistance thermometers (Pt-100s) were used to measure equilibrium temperatures. The Pt-100 temperature probes were calibrated using a silicon oil bath (WIKA CTB 9100) and a WIKA primary temperature probe which was connected to a WIKA CTH 6500 multimeter. The calibration uncertainty was ± 0.03 K. The combined uncertainty in the temperature measurement is ± 0.1 K (k = 2). The pressure in the cylindrical cell was measured using a WIKA pressure transducer which has a pressure limit of 10 MPa. After the calibration of the temperature and pressure sensors, measurements of vapor pressure were undertaken to verify the calibrations and calculated uncertainties. Table 3 reports the vapor pressure data measured in this study. Figure 2 presents the vapor pressure measurements for R507, R134a, R410a, R22, hexafluoropropylene oxide (HFPO) and carbon dioxide (CO_2). There is good agreement between the experimental and literature[22−26] vapor pressures. The combined uncertainty in the reported pressure is ± 0.005 MPa (k = 2).

Experimental Method. The dissociation conditions reported in this study were measured using an isochoric pressure search method.[1−3,17,18] The cell was initially evacuated to 0.2 kPa for a period of 30 min to ensure there was no trace of impurities or contamination from previous experiments. A volume of 10 cm^3 of NaCl aqueous solution was filled into the cell. The cylindrical cell was immersed into the temperature-controlled bath and the refrigerant was supplied from its cylinder through a pressure regulating valve into the cell. The mixture of refrigerant + water + NaCl was left inside the equilibrium cell to allow refrigerant absorption into the solution until the temperature and pressure stabilized. Initially, the system temperature was set outside the hydrate formation region. It was decreased very slowly to allow the formation

dx.doi.org/10.1021/je400067u | J. Chem. Eng. Data XXXX, XXX, XXX−XXX

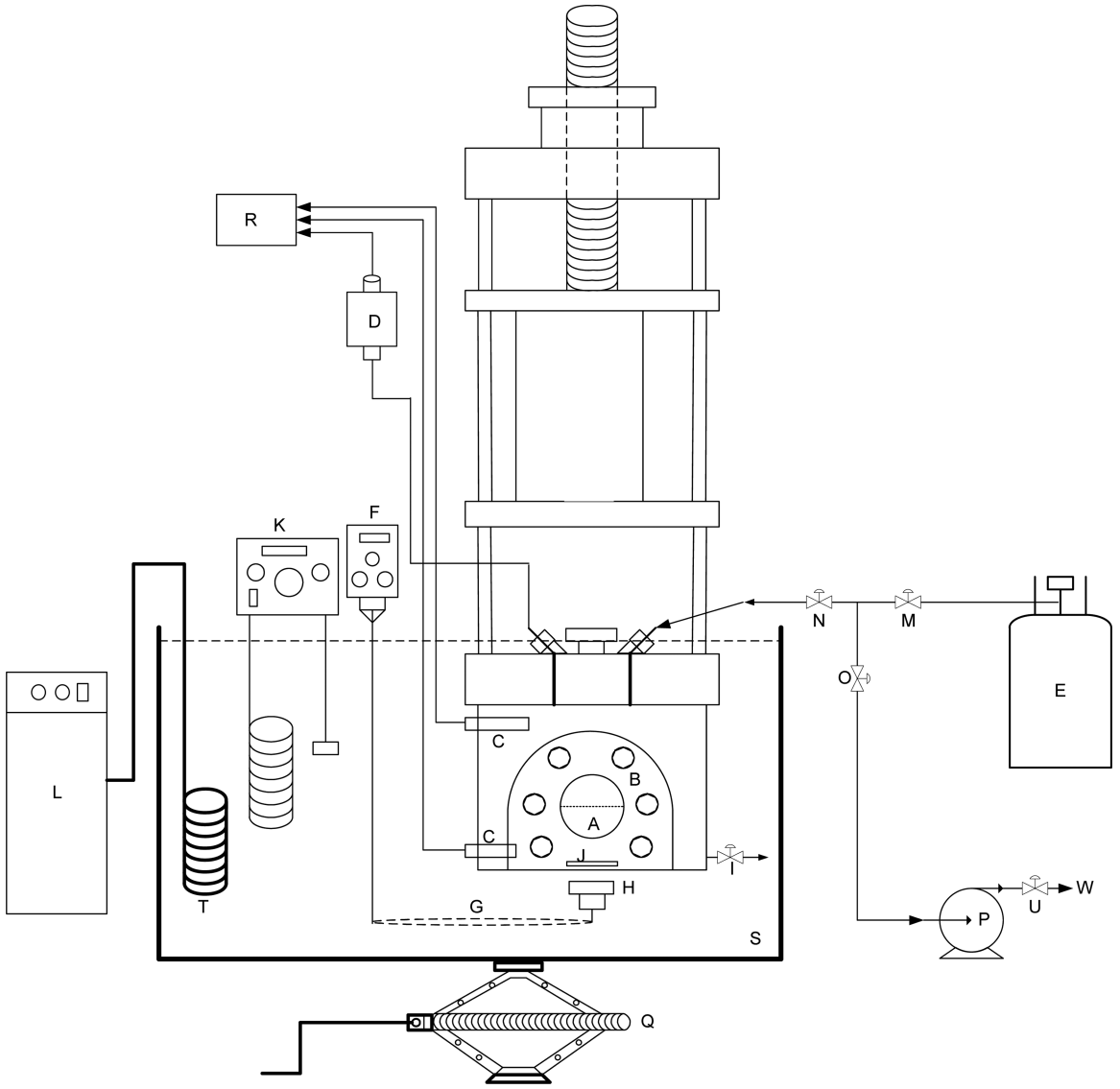

Figure 1. Schematic diagram for the cell:[16] A, sapphire window; B, equilibrium static cell; C, Pt-100; D, pressure transducer; E, refrigerant gas cylinder; F, mechanical stirrer; G, mechanical chain; H, magnetic stirrer; I, drain valve; J, magnetic bar; K, temperature programmable circulator; L, cold finger; M, inlet charging valve; N, control valve; O, control vacuum valve; P, vacuum pump; Q, mechanical jack; R, data acquisition unit; S, water bath with chilling fluid; T, cooling coil; U, vent valve to atmosphere; W, line open to atmosphere.

of gas hydrates. During this hydrate formation stage, a considerable pressure drop was recorded in the cell. After the formation of hydrates, the system temperature was gradually increased. In close proximity to the dissociation point, the temperature incremental step was set to 0.2 K. For each temperature increment of 0.2 K, the time taken to achieve equilibrium was approximately 5 h. A typical hydrate formation and disassociation cycle for the isochoric pressure search method is illustrated in Figure 3. The equilibrium conditions are shown in Figure 4 on an enlarged scale with the corresponding temperatures (T_{eq}) and pressures (P_{eq}) for increments of 0.2 K. As the temperature increases, the pressure also increases as the hydrate undergoes dissociation. This is observed until the disappearance of the last hydrate crystal in the cell as shown in Figures 3 and 4. The exact dissociation point is determined by fitting a polynomial or linear mathematical equation to the equilibrium temperature and pressure readings in the hydrate formation region (A) and outside the formation region (B) as shown in Figures 3 and 4. The dissociation pressure and temperature value is calculated from the intersection of the trend lines from the regions A and B, as shown in Figure 4, and is recorded as the dissociation point.

THERMODYNAMIC MODEL

The liquid (aqueous)−hydrate−vapor equilibrium conditions of a system can be calculated by equating the fugacity of water in aqueous phase, f_w^L, and hydrate phase, f_w^H, ignoring the water content of the gas/vapor phase:[2,3,9,19]

$$f_w^L = f_w^H \tag{1}$$

The fugacity of water in the hydrate phase, f_w^H, is related to the chemical potential difference of water in the filled and empty hydrate cage by the following expression:[2,3,9,19,20,21]

$$f_w^H = f_w^{MT} \exp \frac{\mu_w^H - \mu_w^{MT}}{RT} \tag{2}$$

dx.doi.org/10.1021/je400067u | J. Chem. Eng. Data XXXX, XXX, XXX−XXX

Table 3. Measured Vapor Pressures for Hydrate Formers (Refrigerants) Studied[a,b]

T/K	P/MPa	ΔP/MPa[c,e]	T/K	P/MPa	ΔP/MPa[e]
	R507[c]			R134a[d]	
258.2	0.381	0.002	258.2	0.162	0.002
261.9	0.435	0.002	262.2	0.193	0.000
269.2	0.555	0.002	272.2	0.286	0.003
277.6	0.725	0.002	282.6	0.411	0.004
282.6	0.843	0.001	292.9	0.569	0.002
287.6	0.974	0.001	302.7	0.763	0.004
293.1	1.133	0.002			
297.8	1.287	0.001			
	R410a[f]			R22[g]	
262.5	0.570		273.0	0.495	0.002
271.4	0.758		275.0	0.528	0.002
273.3	0.807		277.0	0.562	0.002
277.6	0.922		285.1	0.718	0.004
282.6	1.070		286.9	0.761	0.002
287.6	1.246		289.0	0.807	0.004
292.6	1.429		283.0	0.677	0.003
297.6	1.635		281.0	0.637	0.003
302.7	1.855		279.0	0.599	0.002
			291.1	0.855	0.005
			295.1	0.955	0.006
	HFPO[h]			CO_2[d]	
293.0	0.588	0.001	283.0	4.406	0.018
288.0	0.505	0.001	273.0	3.387	0.016
283.0	0.431	0.000	293.0	5.627	0.012
278.0	0.366	0.000	298.1	6.323	0.004
273.0	0.309	0.001			
302.9	1.475	0.002			

[a] $U(T) = \pm 0.1$ K ($k = 2$). [b] $U(P) = \pm 0.005$ MPa ($k = 2$). [c] Literature values calculated using

$$P/\text{kPa} = \exp[\ln P_c + (A(1 - T_R) + B(1 - T_R)^{1.5} + C(1 - T_R)^{3.5} + D(1 - T_R)^4)/T_R] \quad \text{(T-I)}$$

[d] Literature values calculated using

$$P/\text{kPa} = \exp[\ln P_c + (A(1 - T_R) + B(1 - T_R)^{1.5} + C(1 - T_R)^{2.5} + D(1 - T_R)^5)/T_R] \quad \text{(T-II)}$$

[e] $$\Delta P = |P_{lit} - P_{exp}| \quad \text{(T-III)}$$

[f] Literature vapor pressure from ref 26.

[g] $$\log(P/\text{bar}) = A - \frac{B}{T/\text{K} + C} \quad \text{(T-IV)}$$

[h] $$P/\text{kPa} = \exp\left[A + \frac{B}{(T/\text{K})} + C\ln(T/\text{K}) + D\cdot 10^{-17}\cdot(T/\text{K})^E\right] \quad \text{(T-V)}$$

where pressure, P/kPa, critical pressure, P_c/kPa, reduce temperature, T_R, temperature, T/K and constants, A, B, C, D, and E are listed in Table 4.

where f_w^{MT} is the fugacity of water in the hypothetical empty hydrate phase, $\mu_w^H - \mu_w^{MT}$ represents the chemical potential of water in the filled (μ_w^H) and empty (μ_w^{MT}) hydrate. R and T stand for universal gas constant and temperature, respectively. The solid solution theory[14] can be used to calculate $(\mu_w^H - \mu_w^{MT})/(RT)$:[2,3,9,19,20]

$$\frac{\mu_w^H - \mu_w^{MT}}{RT} = -\sum_i \nu'_i \ln\left(1 + \sum_j C_{ij} f_j\right) = \sum_i \ln\left(1 + \sum_j C_{ij} f_j\right)^{-\nu'_i} \quad (3)$$

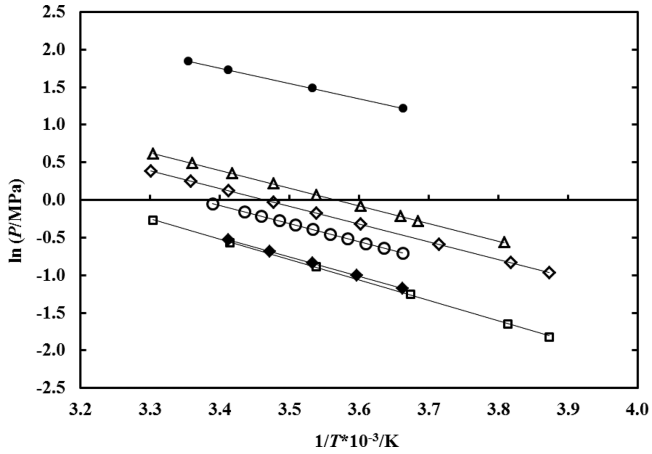

Figure 2. Vapor pressure curve for the refrigerants studied: ○, R22; □, R134a; Δ, R410a; ◊, R507; ♦, HFPO; ●, CO_2; −, literature.[22−24,26]

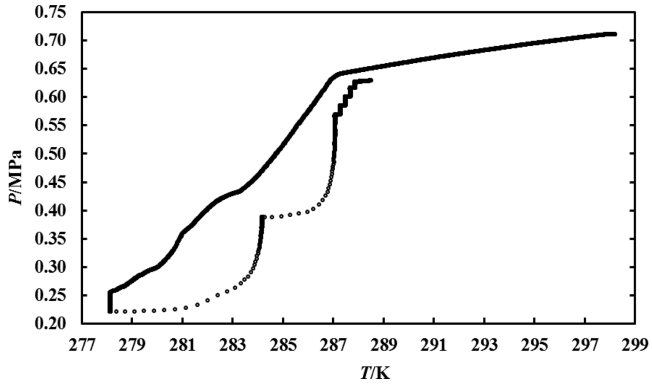

Figure 3. Typical formation and dissociation hydrate curves for the R22 (1) + water (2) System: ●, hydrate formation and dissociation points.

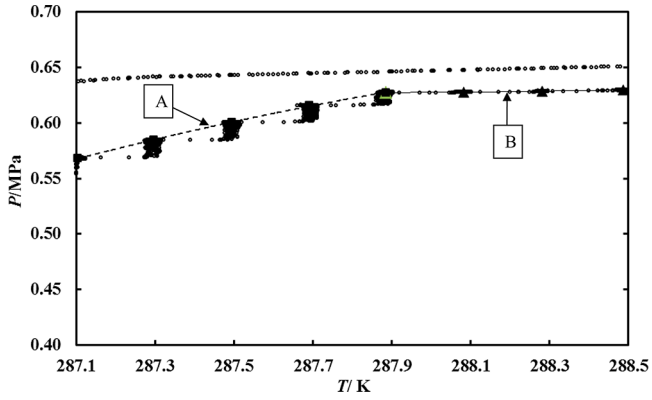

Figure 4. Typical analysis for the determination of hydrate dissociation point for the R22 (1) + water (2) system: ●, hydrate formation and dissociation; ---, A (hydrate formation region, −, B (outside the hydrate formation region).

dx.doi.org/10.1021/je400067u | J. Chem. Eng. Data XXXX, XXX, XXX−XXX

Table 4. Constants for Equations 13, T-I, T-II, T-IV, and T-V

	A	B	C	D	E
NaCl[a]	$-1.191\cdot10^{01}$	$1.037\cdot10^{-02}$	$-6.043\cdot10^{-02}$	$-5.814\cdot10^{-03}$	$3.861\cdot10^{-04}$
R507[b]	−7.342584	1.046268	1.999693	−9.207652	
R134a[c]	−7.6485	1.788344	−2.633842	−3.355961	
CO_2[c]	−7.019137	1.48658	−2.048273	−5.324421	
R22[d]	4.13253	835.4620	243.460		
HFPO[e]	53.1702	−3799.8834	−4.7530	12.3069	6.000

[a]Reference 33. [b]Reference 23. [c]Reference 24. [d]Reference 22. [e]Reference 26.

where v_i' is the number of cavities of type i per water molecule in a unit hydrate cell, C_{ij} stands for the Langmuir constant for the hydrate former's interaction with each type of cavity and f_j is the fugacity of hydrate former.[2,3,9,19,20] The fugacity of water in the hypothetical empty hydrate phase can be expressed as:[2,3,9,19,20]

$$f_w^{MT} = P_w^{MT}\varphi_w^{MT}\exp\int_{P_w^{MT}}^{P}\frac{v_w^{MT}\,dP}{RT} \quad (4)$$

where P_w^{MT} is the vapor pressure of the empty hydrate lattice, φ_w^{MT} is the correction for the deviation of the saturated vapor of pure lattice from ideal behavior, and v_w^{MT} is the partial molar volume of water in the empty hydrate.[9] The exponential term is a Poynting correction.

Two assumptions can be made in eq 4: (1) The hydrate partial molar volume equals to the molar volume and is independent of pressure. (2) P_w^{MT} is relatively small (in the order of 10^{-3} MPa), therefore $\varphi_w^{MT} = 1$.

Therefore, eq 4 can be simplified to[2,3,9,19,20]

$$f_w^{MT} = P_w^{MT}\exp\frac{v_w^{MT}(P - P_w^{MT})}{RT} \quad (5)$$

By substitution of eq 5 into eq 2, the fugacity of water in the hydrate phase can be expressed by[9]

$$f_w^{H} = P_w^{MT}\exp\left[\frac{v_w^{MT}(P - P_w^{MT})}{RT}\right] \times [(1 + C_{small}f^{V}_{refrigerant})^{-\nu'_{small}}(1 + C_{large}f^{V}_{refrigerant})^{-\nu'_{large}}] \quad (6)$$

where $f^{V}_{refrigerant}$ is the fugacity of refrigerant hydrate former in the vapor. The subscripts "small" and "large" refer to the small and large cavities, respectively. The Poynting correction term can be considered in calculations if the dissociation pressure is greater than 2 MPa. In this study, the Poynting correction term was ignored. The dissociation pressures of gas hydrates of refrigerants are lower than 2 MPa,[4,5,9,10,27−35] hence it was assumed that the fugacity of refrigerants in the vapor phase is equal to the dissociation pressure of gas hydrate and it was assumed that the vapor phase is ideal gas of refrigerant.[9] Therefore, $f^{V}_{refrigerant} = P$ and the fugacity of water in hydrate phase can be expressed as[9]

$$f_w^{H} = P_w^{MT}[(1 + C_{small}P)^{-\nu'_{small}}(1 + C_{large}P)^{-\nu'_{large}}] \quad (7)$$

The vapor pressure of the empty hydrate lattice, P_w^{MT}, is calculated by equating the fugacity of water in the hydrate phase to that of pure ice at the three−phase line.[3] Sloan[3] reported the equations for the vapor pressure of the empty hydrate structure, and the values of the number of cavities, v_i' of type i per water molecule in a unit hydrate cell for structure I and for structure II are found in literature.[2,3,9,14,19]

The Langmuir constants account for interactions between the hydrate former and water molecules in the cativies[21] for a range of temperatures and hydrates formers.[3,9] The integration procedure for determining the Langmuir constants for the temperature range uses the Kihara potential function with a spherical core.[3,9] In the study, the model parameters for Langmuir constants for hydrate formers interaction with each type of cavity has been determined using the eqs 8 and 9.[2,3,9,19,21]

For a small cavity (pentagonal dodecahedral)

$$C_{small} = \frac{a}{T}\exp\left(\frac{b}{T}\right) \quad (8)$$

and for a large cavity (tetrakaidecahedra (sI) and hexakaidecahedra (sII))

$$C_{large} = \frac{c}{T}\exp\left(\frac{d}{T}\right) \quad (9)$$

where T is in K and C has units of reciprocal MPa. The optimum value of the constants a to d are evaluated by fitting the thermodynamic model to the experimental hydrate dissociation data.[3,21]

Saline Aqueous Phase. Aasberg-Peterson et al.[13] presented a model which can be used to calculate the solubility of gas in aqueous electrolyte solutions. The liquid phase is first treated as a salt-free mixture and an equation of state (EOS) approach is used to describe it. The fugacity coefficient which is computed by the EOS is corrected by the Debye−Huckel electrostatic term. This term depends on the ionic strength of the solution and hence on the electrolyte concentration. It also depends on the type of the electrolyte through an adjustable parameter which is dependent of temperature and composition.

The fugacities in the aqueous phase that contains the electrolytes are calculated from the equation:[3,13,22,33]

$$f_w^{L} = x_w\phi_w^{L}P \quad (10)$$

Table 5. Experimental Data for the Dissociation Conditions of Gas Hydrates for the R22 (1) + Water (2) System with Comparison to Literature[a,b]

R22 (1) + water (2)		literature[c]	literature[d]	literature[e]
T/K	P/MPa	ΔP/MPa[f]	ΔP/MPa[f]	ΔP/MPa[f]
278.9	0.181	0.002	0.003	0.007
282.2	0.293	0.005	0.010	0.007
283.6	0.350	0.005	0.014	0.006
285.7	0.468	0.003	0.008	0.013
286.9	0.535	0.004	0.011	0.015
287.8	0.630	0.006	0.008	0.015
288.3	0.645	0.004	0.006	0.013

[a]$U(T) = \pm 0.1$ K ($k = 2$). [b]$U(P) = \pm 0.005$ MPa ($k = 2$). [c]Reference 29. [d]Reference 30., and. [e]Reference 31. [f]$\Delta P = |P_{lit} - P_{exp}|$

dx.doi.org/10.1021/je400067u | J. Chem. Eng. Data XXXX, XXX, XXX−XXX

where the fugacity coefficient of the aqueous phase is given by the model as follows[13,33]

$$\ln \phi_w^L = \ln \phi^{EOS} + \ln \gamma^{EL} \quad (11)$$

where γ^{EL} accounts for the effect of the electrolytes. For a system that contains electrolytes a correction term is added to account for the electrostatic interactions. The effect of the electrolytes is given by the following expression[13,33]

$$\ln \gamma^{EL} = \frac{2A' h_{is} M_m F(B' I^{0.5})}{B'^3} \quad (12)$$

where h_{is} is an interaction coefficient between the dissolved salt and a noneletrolytic component. This coefficient is dependent on temperature, composition, and ionic strength (I). M_m is the salt-free mixture molecular weight determined as a molar average. Tohidi et al.[33] calculated h_{is} for a number of water−electrolyte and gas−electrolyte systems

$$h_{is} = \frac{A + BT + Cx + Dx^2 + ETx}{1000} \quad (13)$$

The parameters A' and B', as well as the function F in eq 12 are given by the following equations:[13,33]

$$A' = 1.327757 \cdot 10^5 \left(\frac{d_m^{0.5}}{(\varepsilon_m T)^{0.5}} \right) \quad (14)$$

$$B' = 6.359696 \left(\frac{d_m^{0.5}}{(\varepsilon_m T)^{0.5}} \right) \quad (15)$$

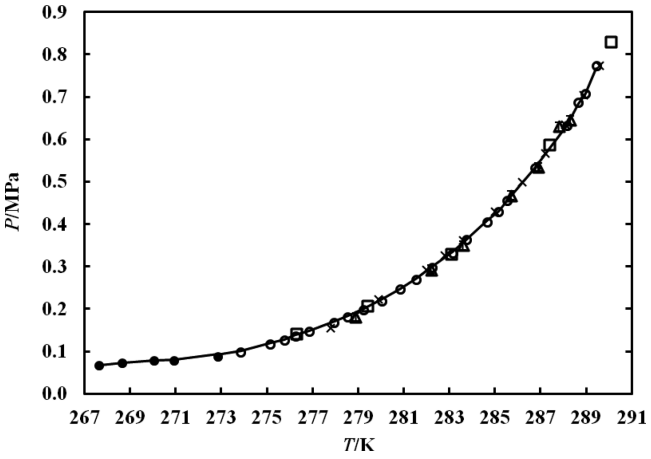

Figure 5. Comparison between the experimental hydrate dissociation data and the model result of Eslamimanesh et al.[9] for the R22 (1) + water (2) system: Δ, measured with error bars of 0.005 MPa; ○, literature;[29] × , literature;[30] □, literature;[31] ——, model.

Table 6. Experimental Data for the Dissociation Conditions of Gas Hydrate for the R134a (1) + Water (2) + NaCl (3) System at Varying Concentrations of Salt.[a,b]

R134a (1) + water (2)		R134a (1) + water (2) + 0.900 mol·kg^{-1} NaCl (3)		R134a (1) + water (2) + 1.901 mol·kg^{-1} NaCl (3)	
T/K	P/MPa	T/K	P/MPa	T/K	P/MPa
283.0	0.428	280.6	0.383	277.1	0.340
282.8	0.400	280.5	0.371	277.1	0.337
282.4	0.368	280.0	0.330	276.7	0.309
282.2	0.350	279.2	0.280	276.1	0.261
281.6	0.308	278.9	0.263	275.7	0.238
281.0	0.269	278.2	0.222	275.0	0.202
280.5	0.236	278.0	0.211	274.8	0.189
279.2	0.180	277.4	0.180	274.3	0.173
278.4	0.150	276.5	0.147	273.7	0.148
277.1	0.114	275.2	0.110	273.3	0.138
		274.6	0.098	272.6	0.117
R134a (1) + water (2) + 3.020 mol·kg^{-1} NaCl (3)					
	273.4				0.299
	272.8				0.257
	271.0				0.176
	269.6				0.128
	268.6				0.096
	268.1				0.086

[a] $U(T) = \pm 0.1$ K ($k = 2$). [b] $U(P) = \pm 0.005$ MPa ($k = 2$).

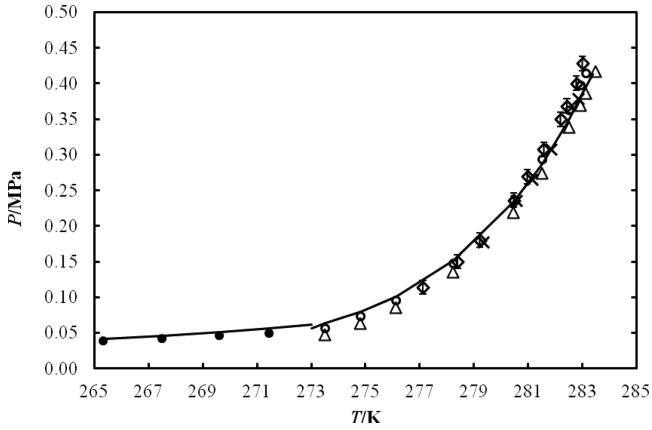

Figure 6. Comparison between the experimental hydrate dissociation data and the model result of Eslamimanesh et al.[9] for the R134a (1) + water (2) system: ◇, measured with error bars of 0.005 MPa; ○, literature;[27] Δ, literature;[28] × , literature;[34] ——, model.

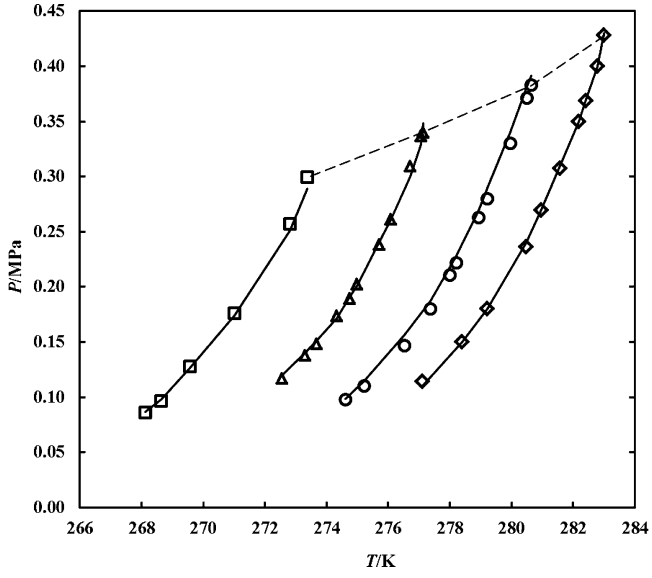

Figure 7. Experimental and calculated hydrate dissociation pressures for the R134a (1) + water (2) + NaCl (3) system; ◇, no salt; ○, 0.900 mol·kg^{-1}; Δ, 1.901 mol·kg^{-1}; □, 3.020 mol·kg^{-1}; ——, model; ---, quadruple point line.

dx.doi.org/10.1021/je400067u | J. Chem. Eng. Data XXXX, XXX, XXX−XXX

$$F(B'I^{0.5}) = 1 + B'I^{0.5} - \frac{1}{1 + B'I^{0.5}} - 2\ln(1 + B'I^{0.5}) \quad (16)$$

where d_m is the density of the salt-free mixture and is assumed to be equal to the density of water. The quantity ε_m is the salt-free mixture dielectric constant which for a mixture of gases and water is given by[13,33]

$$\varepsilon_m = x_N \varepsilon_N \quad (17)$$

where x_N and ε_N are salt-free mole fraction and the dielectric constant of water:[13,33]

$$\varepsilon_N = 305.7 \exp\left(-\exp(-12.741 + 0.01875T) - \frac{T}{219}\right) \quad (18)$$

RESULTS AND DISCUSSION

The binary system R22 + water was measured and compared with data from literature.[29−31] The experimental data is shown in Table 5 and plotted in Figure 5. Table 6 and Figure 6 present the measured binary data for the R134*a* + water system, which is compared with data from literature.[27,28,34] These two systems were initially measured to evaluate the reliability of the isochoric pressure-search method[1−3,17,18,34] for the determination of gas hydrate dissociation data. To the best of our knowledge there is no experimental data for the hydrate−liquid water−vapor (H−L_w−V) equilibria for the R134a + NaCl + water system at varying salt concentrations, viz. (0.900, 1.901, and 3.020) mol·kg^{-1}. The ternary data measured are listed in Table 6 and shown in Figure 7.

There also appears to be no data available in the literature for hydrate−liquid water−vapor equilibria for the refrigerants R507 and R410a. Gas hydrate dissociation data for the binary systems {R507 or R410a} + water and ternary systems of {R507 or R410a} + NaCl + water at salt concentrations of (0.900 and 1.901) mol·kg^{-1} are presented in Tables 7 and 8 and plotted in Figures 8 and 9, respectively. As can be seen from the measured data, the addition of NaCl to the {R134a or R507 or R410a} + water systems causes an inhibition of the H−L_w−V equilibrium phase boundary with its shifting to lower temperatures as molality increases, as indicated in Figures 7 to 9. In the presence of the

Table 7. Experimental Data for the Dissociation Conditions of Gas Hydrate for the R507 (1) + Water (2) + NaCl (3) System at Varying Concentrations of Salt[a,b]

R507 (1) + water (2)		R507 (1) + water (2) + 0.900 mol·kg^{-1} NaCl (3)		R507 (1) + water (2) + 1.901 mol·kg^{-1} NaCl (3)	
T/K	*P*/MPa	*T*/K	*P*/MPa	*T*/K	*P*/MPa
282.8	0.549	281.4	0.625	279.3	0.656
282.2	0.492	280.8	0.554	278.4	0.551
281.2	0.398	280.5	0.529	277.7	0.493
281.2	0.398	279.8	0.469	277.2	0.439
279.9	0.319	279.4	0.430	276.6	0.391
279.2	0.269	278.5	0.360	275.7	0.329
278.2	0.224	277.7	0.317	275.1	0.289
277.1	0.183	276.9	0.269		
276.4	0.159				

[a] U(T) = ± 0.1 K (k = 2). [b] U(P) = ± 0.005 MPa (k = 2).

Table 8. Experimental Data for the Dissociation Conditions of Gas Hydrate for the R410a (1) + Water (2) + NaCl (3) System at Varying Concentrations of Salt.[a,b]

R410a (1) + water (2)		R410a (1) + water (2) + 0.900 mol·kg^{-1} NaCl (3)		R410a (1) + water (2) + 1.901 mol·kg^{-1} NaCl (3)	
T/K	*P*/MPa	*T*/K	*P*/MPa	*T*/K	*P*/MPa
291.8	1.106	290.3	1.112	289.1	1.170
290.7	0.947	289.2	0.956	288.2	1.047
289.9	0.827	288.2	0.838	287.3	0.927
289.2	0.743	287.0	0.726	286.3	0.831
288.2	0.644	285.7	0.603	284.6	0.663
287.5	0.586	284.4	0.507	282.3	0.494
286.3	0.489	282.5	0.389	280.7	0.398
285.6	0.436	280.5	0.287	280.2	0.371
284.4	0.365			278.8	0.303
283.5	0.312				
281.9	0.252				
281.2	0.226				

[a] U(T) = ± 0.1 K (k = 2). [b] U(P) = ± 0.005 MPa (k = 2).

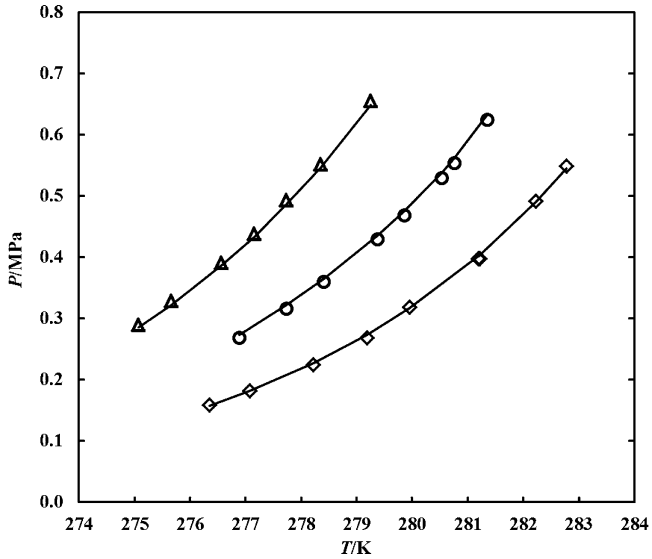

Figure 8. Experimental and calculated hydrate dissociation pressures for the R507 (1) + water (2) + NaCl (3) system; ◇, no salt; ○, 0.900 mol·kg^{-1}; Δ, 1.901 mol·kg^{-1}; ——, model.

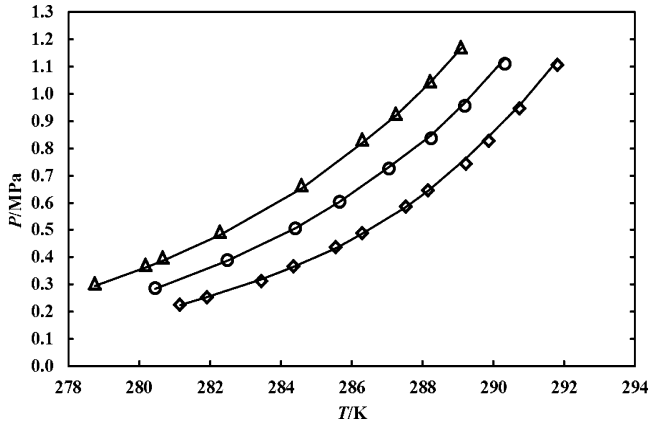

Figure 9. Experimental and calculated hydrate dissociation pressures for the R410a (1) + water (2) + NaCl (3) system; ◇, no salt; ○, 0.900 mol·kg^{-1}; Δ, 1.901 mol·kg^{-1}; ——, model.

dx.doi.org/10.1021/je400067u | J. Chem. Eng. Data XXXX, XXX, XXX−XXX

electrolyte, refrigerant solubility decreases because the interactions between the water molecules and the ions are stronger than the interactions between the water and the dissolved refrigerant (salting out effect). It was found that the system of R134a + water + NaCl exhibited a quadruple point, a condition at which the four phases ($H-L_w-L_{R134a}-V$) coexist.

The use of a refrigerant in hydrate technology for desalination or wastewater treatment is promising because it forms a hydrate with water only.[3,4,6−8,10,12] As a result, when the gas hydrate dissociates, pure water is produced and the refrigerant is released. The refrigerant is recycled for reuse.[3,4,6−8,10,12] In this study, it was revealed that by comparing the dissociation conditions, R410a could be the most suitable refrigerant (among the refrigerants studied in the present work) that may be used in the desalination process because the hydrate dissociation temperatures are close to ambient conditions, while R507 and R134a may require a water insoluble promoter in order to shift the temperatures close to ambient conditions.

The measured systems are modeled using the approach explained earlier. The Langmuir parameters (a, b, c, and d) were obtained by using eqs 8 and 9 in the absence of salt. Thereafter, the constants were regressed to adjust the parameters in eq 13 using hydrate dissociation points in the presence of NaCl aqueous solutions. The Langmuir parameters for the refrigerant blends, R410a, and R507, were obtained with the assumption that they are pure gases. All adjustable parameters of the models were obtained by minimizing the following objective function (OF) or average absolute deviation (AAD):

$$\mathrm{OF} = \frac{100}{N}\sum_{i}^{N}\frac{|P_i^{\mathrm{cal}} - P_i^{\mathrm{exp}}|}{P_i^{\mathrm{exp}}} \tag{19}$$

where N is number of data points used in the optimization procedure, subscript i stands for ith calculated or experimental hydrate dissociation point and the superscripts "cal" and "exp" refer to calculated and experimental hydrate dissociation points, respectively. Table 9 presents the Langmuir constants for the refrigerant + water systems in this study. It can be seen from Table 9 that the Langmuir constants and AAD of the R134a + water system compare favorably with those of Eslamimanesh et al.[9] Previous studies[9,27,35] show that R134a forms hydrates of type sII with large cavities. R134a, R410a, and R507 are large molecules which cannot enter the small cavities of their relevant gas hydrate structures, while R22 molecules can occupy large cavities of sI, as indicated by Chun et al.[10] Equation 9 was used to obtain Langmuir constants for large cavities of structure type sI and sII. As can be observed, the model results agree satisfactorily with experimental hydrate dissociation data demonstrating the ability of the model to describe the hydrate phase behavior.

Table 9. Regressed Langmuir Constants for Refrigerant Gas Hydrate Systems with Salt in this Study

hydrate former	a	b	c	d	AAD[a]
R134a	0.00	0.00	$5.70\cdot10^{-3}$	4908.71	5.30
R410a	0.00	0.00	$4.15\cdot10^{-6}$	7865.12	1.07
R507	0.00	0.00	$2.65\cdot10^{-6}$	7728.00	0.83
R22	0.00	0.00	$3.5\cdot10^{-5}$	5576.53	0.08

[a]AAD (%) = $(100/N)\sum_i^N((|P_i^{\mathrm{cal}} - P_i^{\mathrm{exp}}|)/P_i^{\mathrm{exp}})$.

CONCLUSIONS

Experimental hydrate dissociation data for systems involving water + {R22 or R410a, or R507 or R134a} in the absence and presence of NaCl were measured at various molalities of the salt. The R134a + water + NaCl system was measured at salt concentrations of (0.900, 1.901, and 3.020) mol·kg^{-1}, while the {R410a or R507} + water + NaCl system was measured at salt concentrations of (0.900 and 1.901) mol·kg^{-1}. The binary system of R22 + water was measured in the absence of salt. A quadruple point at which the four phases ($H-L_w-L_{R134a}-V$) coexist was determined for the water + R134a + NaCl system. The isochoric pressure-search method[1−3,17,18,34] was used for the hydrate dissociation measurements. This preliminary study indicates that R507 and R134a would not be suitable for application in gas hydrate technology. A water insoluble promoter is probably required which when added to the {R507 or R134a} + water + NaCl system would shift the $H-L_w-V$ equilibrium phase boundary closer to ambient conditions. The presence of NaCl salt in the aqueous solutions exhibited a thermodynamic inhibition effect on the refrigerant gas hydrates, in which the $H-L_w-V$ equilibrium phase boundary is shifted to low dissociation temperatures. The experimental dissociation data were satisfactorily modeled with a combination of the Aasberg-Petersen et al.[13] model for electrolyte aqueous systems with the solid solution theory of van der Waals and Platteeuw[14] used to model the hydrate phase and the Peng−Robinson[15] equation of state with classical mixing rule used for the aqueous/liquid and vapor phases.

AUTHOR INFORMATION

Corresponding Author

*E-mail: ramjuger@ukzn.ac.za; a.h.m@irgcp.fr.

Funding

This work is based upon research supported by the South African Research Chairs Initiative of the Department of Science and Technology and National Research Foundation. The authors would like to thank the NRF Focus Area Programme and the NRF Thuthuka Programme.

Notes

The authors declare no competing financial interest.

REFERENCES

(1) Mohammadi, A. H.; Richon, D. Phase equilibria of methane hydrates in the presence of methanol and/or ethylene glycol aqueous solution. *Ind. Eng. Chem. Res.* **2010**, *49*, 925−928.

(2) Tumba, K.; Reddy, P.; Naidoo, P.; Ramjugernath, D.; Eslamimanesh, A.; Mohammadi, A. H.; Richon, D. Phase equilibria of methane and carbon dioxide clathrate hydrates in the presence of aqueous solutions of tributylmethlyphosphonuim methylsulfate ionic liquid. *J. Chem. Eng. Data* **2011**, *56*, 3620−3629.

(3) Sloan, E. D.; Koh, C. A. *Clathrate Hydrates of Natural Gases*, 3rd ed.; CRC Press, Taylor & Francis Group: London, NY, 2008.

(4) Javanmaardi, J.; Moshefeghian, M. Energy consumption and economic evaluation of water desalination by hydrate phenomenon. *Appl. Therm. Eng* **2003**, *23*, 845−857.

(5) Huang, C. P.; Fennema, O.; Poweri, W. D. Gas hydrates in aqueous-organic systems: II. Concentration by gas hydrate formation. *Cryobiology* **1966**, *2*, 240−245.

(6) Khawaji, A. D.; Kutubkhanaha, I. K.; Wie, J.-M. Advances in seawater desalination technologies. *Desalination* **2008**, *221*, 47−69.

(7) Park, K.; Hong, S. Y.; Lee, J. W.; Kang, K. C.; Lee, Y. C.; Ha, M.-G.; Lee, J. D. A new apparatus for seawater desalination by gas hydrate process and removal characteristics of dissolved minerals. *Desalination* **2011**, *274*, 91−96.

(8) Kalogirou, S. A. Seawater desalination using renewable energy sources. *Prog. Energy Combust. Sci.* **2005**, *31*, 242−281.
(9) Eslamimanesh, A.; Mohammadi, A. H.; Richon, D. Thermodynamic model for predicting phase equilibria of simple clathrate hydrates of refrigerants. *Chem. Eng. Sci.* **2011**, *66*, 5439−5445.
(10) Chun, M.-K.; Lee, H.; Ryu, B. J. Phase equilibria of R22 ($CHClF_2$) hydrate systems in the presence of NaCl, KCl and $MgCl_2$. *J. Chem. Eng. Data* **2000**, *45*, 1150−1153.
(11) Seo, Y.; Lee, H. A new hydrate-based recovery process for removing chlorinated hydrocarbons from aqueous solutions. *Environ. Sci. Technol.* **2001**, *35*, 3386−3390.
(12) Eslamimanesh, A.; Mohammadi, A. H.; Richon, D.; Naidoo, P.; Ramjugernath, D. Application of gas hydrate formation in separation processes: A review of experimental studies. *J. Chem. Thermodyn.* **2012**, *46*, 62−71.
(13) Aasberg-Petersen, K.; Stenby, E.; Fredenslund, A. Prediction of high pressure gas solubilities in aqueous mixtures of electrolytes. *Ind. Eng. Chem. Res.* **1991**, *30*, 2180−2185.
(14) Van der Waals, J. H.; Platteeuw, J. C. Clathrate Solutions. *Adv. Chem. Phys* **1959**, *2*, 1−57.
(15) Peng, D. Y.; Robinson, D. B. A new two constant equation of state. *Ind. Eng. Chem. Fundam* **1976**, *15*, 59−64.
(16) Tshibangu, M. M. *Measurements of HPVLE data for fluorinated systems*. MSc Thesis, Chemical Engineering, University of Kwa-Zulu Natal, 2010.
(17) Afzal, W.; Mohammadi, A. H.; Richon, D. Experimental measurements and predictions of dissociation conditions for methane, ethane, propane, and carbon dioxide simple hydrates in the presence of diethylene glycol aqueous solutions. *J. Chem. Eng. Data* **2008**, *53*, 663−666.
(18) Mohammadi, A. H.; Afzal, W.; Richon, D. Gas hydrate of methane, ethane, propane and carbon dioxide in the presence of single NaCl, KCl and $CaCl_2$ aqueous solutions: Experimental measurements and predictions of dissociation conditions. *J. Chem. Thermodyn.* **2008**, *40*, 1693−1697.
(19) Mohammadi, A. H; Richon, D. Development of predictive techniques for estimating liquid water-hydrate equilibrium of water-hydrocarbon system. *J. Thermodyn.* **2009**, 1−12.
(20) Dharmawardhana, P. B; Parrish, W. R; Sloan, E. D. Experimental thermodynamics parameters for the prediction of natural gas hydrate dissociation conditions. *Ind. Eng. Chem. Fundam.* **1980**, *19* (4), 410−414.
(21) Parrish, W. R.; Prausnitz, J. M. Dissociation pressures of gas hydrates formed by gas mixtures. *Ind. Eng. Chem. Process Des. Dev.* **1972**, *11* (1), 26−35.
(22) Poling, B. E; Prausnitz, J. M; O'Connell, J. P. *The Properties of Gases and Liquids*, 5th ed.; McGraw-Hill: New York, 2001.
(23) Döring, R.; Buchwald, H.; Hellmann, J. Results of experimental and theoretical studies of the azeotropic refrigerant R507. *Int. J. Refrig.* **1997**, *20* (2), 78−84.
(24) *Aspen Plus Version V7.3*; Aspen Technology Inc.: Nashua, NH, 2011.
(25) Calm, J. E. Properties and efficiencies of R-410A, R-421A, R-422B and R-422D compared to R-22. *Refrig. Manage. Serv.* **2008**, 1−14.
(26) Dicko, M.; Belaribi-Boukais, G.; Coquelet, C.; Valtz, A.; Brahim, B. F; Naidoo, P.; Ramjugernath, D. Experimental measurement of vapor pressures and densities at saturation of pure hexafluoropropylene oxide: Modelling using a Crossover equation of state. *Ind. Eng. Chem. Res.* **2011**, *50*, 4761−4768.
(27) Liang, D.; Guo, K.; Wang, R.; Fan, S. Hydrate equilibrium data of 1,1,1,2-tetrafluoroethane (HFC-134a), 1,1-dichloro-1-fluoroethane (HCFC-141b) and 1,1-difluoroethane (HFC-152a). *Fluid Phase Equilib.* **2001**, *187*−*188*, 61−70.
(28) Akiya, T.; Shimazaki, T.; Oowa, M.; Matsuo, M.; Yoshida, Y. Formation conditions of clathrates between HFC alternative refirgerants and water. *Int. J. Thermophys.* **1999**, *20*, 1753−1763.
(29) Wittstruck, T. A; Brey, W. S; Buswell, A. M; Rodebush, W. H. Solid hydrates of some halomethane. *J. Chem. Eng. Data* **1961**, *6*, 343−346.
(30) Javanmardi, J.; Ayatollahi, S.; Motealleh, R.; Moshfeghian, M. Experimental measurement and modeling of R22 (CHClF2) hydrates in mixtures of acetone + water. *J. Chem. Eng. Data* **2004**, *49*, 886−889.
(31) Chun, M-K; Yoon, J-H; Lee, H. Clathrate phase equilibria for the water + deuterium oxide + carbon dioxide and water + deuterium oxide + chlorodifluoromethane (R22) systems. *J. Chem. Eng. Data* **1996**, *41*, 1114−1116.
(32) Englezos, P. Computation of the incipient equilibrium carbon dioxide hydrate formation condition in aqueous solutions. *Ind. Eng. Chem. Res.* **1992**, *31*, 2232−2237.
(33) Tohidi, B.; Danesh, A.; Todd, A. C. Modeling single and mixed electrolyte solutions and its applications to gas hydrates. *Inst. Chem. Eng.* **1995**, *71*, 464−471.
(34) Mohammadi, A. H; Richon, D. Pressure temperature phase diagrams of clathrate hydrates of HFC-134a, HFC-152a and HFC-32, *AIChE Annual Meeting*, 2010, Proceeding, Salt Lake City, UT.
(35) Hashimoto, S.; Miyauchi, H.; Inoue, Y.; Ohgaki, K. Thermodynamic and Raman spectropic studies on difluoroethane (HFC-32) + water binary system. *J. Chem. Eng. Data* **2010**, *55*, 2764−2768.